Comparative Biochemistry and Physiology, Part A 157 (2010) 382–391

Contents lists available at ScienceDirect

Comparative Biochemistry and Physiology, Part A

journal homepage: www.elsevier.com/locate/cbpa

# Onset and early development of hypoxic ventilatory responses and branchial neuroepithelial cells in *Xenopus laevis*

Tien-Chien F. Pan *, Warren W. Burggren

*Developmental Physiology and Genetics Research Cluster, Department of Biological Sciences, University of North Texas, Denton, Texas 76203-5017, USA*

ARTICLE INFO

*Article history:*
Received 25 May 2010
Received in revised form 9 August 2010
Accepted 10 August 2010
Available online 20 August 2010

*Keywords:*
Control of breathing
Development
Hypoxia
Neuroepithelial cell
Ventilation
*Xenopus laevis*

ABSTRACT

Onset and ontogeny of the $O_2$ chemoreceptive control of ventilation was investigated in *Xenopus laevis*. The density and size of branchial serotonin-immunoreactive neuroepithelial cells (5-HT-IR NECs) were also determined using confocal immunofluorescent microscopy. Larvae started gill ventilation at 3 days post-fertilization (dpf), and, at this early stage, acute hypoxic exposure produced an increase in frequency from $28 \pm 4$ to $60 \pm 2$ beats·min$^{-1}$. Concurrent with the onset of ventilatory responses, 5-HT-IR NECs appeared in the gill filament bud. Lung ventilation began at 5 dpf and exhibited a 3-fold increase in frequency during acute hypoxia. At 10 dpf, gill ventilatory sensitivity to hypoxia increased, as did NEC density, from $15 \pm 1$ (5 dpf) to $29 \pm 2$ (10 dpf) cells·mm of filament$^{-1}$. Unlike ventilation frequency, gill ventilation amplitude and lung expired volume were unaltered by acute hypoxia. Chronic exposure to moderate hypoxia, at a $P_{O_2}$ of 110 mmHg, attenuated acute responses to moderate hypoxia at 10 and 14 dpf but had no effect at more severe hypoxia or at other stages. Chronic hypoxia also stimulated 5-HT-IR NECs growth at 21 dpf. Collectively, larvae at 5 dpf exhibited strong $O_2$-driven gill and lung ventilatory responses, and between 10 and 21 dpf, the early hypoxic responses can be shaped by the ambient $P_{O_2}$.

Published by Elsevier Inc.

## 1. Introduction

The dramatic shift from primarily water breathing to primarily air breathing during development in amphibians has attracted special attention from respiratory physiologists (e.g. Malvin, 1989; Burggren and Just, 1992; Wang et al., 1999; Jonz and Nurse, 2006; Gargaglioni and Milsom, 2007; Burggren and Warburton, 2007; Burggren and Pan, 2009; Kinkead, 2009). Buccal pumping behavior starts less than a day after hatching in most anurans, producing water flow through the buccopharyngeal water passage and branchial chambers (Nieuwkoop and Faber, 1967; Feder and Wassersug, 1984). However, during this early period of development, anuran larvae still acquire $O_2$ primarily via the skin and the external gills, which may not be directly ventilated by buccal pumping (Feder and Burggren, 1987; Burggren and Just, 1992). In larval *Xenopus laevis*, the external gills degenerate within a day after the onset of gill ventilation coincident with the appearance of the developing internal gills (Nieuwkoop and Faber, 1967). The overall distribution of gas exchange between these organs has not been studied in early larval *Xenopus*. However, in *Lithobates catesbeianus* (formerly *Rana catesbeiana*), the internal gills are responsible for about 40% of the total $O_2$ uptake, with the rest via the skin during early development (Burggren and West, 1982).

The lungs of anuran amphibians also begin to develop shortly after hatching. In both *X. laevis* and *Lithobates catesbeianus*, larvae start air-breathing around the time that buccal pumping behavior starts (Burggren and Doyle, 1986; Pronych and Wassersug, 1994). Despite early filling of the lungs with air, aerial $O_2$ uptake may not make significant contributions to gas exchange, since blood vessels around the lung epithelium are not evident until approximately 21 dpf in *X. laevis* (Nieuwkoop and Faber, 1967). Instead, early development of lung ventilation may be necessary for the regulation of buoyancy and stimulation of lung development (Wassersug and Feder, 1983; Feder and Wassersug, 1984; Feder et al., 1984; Wassersug and Murphy, 1987). With the gradual maturation of the lungs as development progresses, the relative importance of internal gills decreases and accounts for less than 20% of total $O_2$ uptake before metamorphosis (Burggren and West, 1982).

Given these ontogenic changes in amphibian gas exchange organs, not surprisingly, ventilatory regulation also changes in a complex manner. In early larval stages, amphibians respond to aquatic hypoxia mainly by increasing buccal pumping frequency, a behavior that effectively increases irrigation of the internal gills (West and

*Abbreviations:* 5-HT, 5-hydroxytryptamine or serotonin; dpf, days post-fertilization; $f_G$, gill ventilation frequency; $f_L$, lung ventilation frequency; NEC, neuroepithelial cell; $P_{O_2}$, partial pressure of oxygen.

* Corresponding author. Department of Biological Sciences, University of North Texas, 1155 Union Circle, #305220, Denton, Texas 76203-5017, USA. Tel.: +1 940 565 3595; fax: +1 940 565 3821.
*E-mail address:* francispan@my.unt.edu (T.-C.F. Pan).

1095-6433/$ – see front matter. Published by Elsevier Inc.
doi:10.1016/j.cbpa.2010.08.018

Burggren, 1982; Feder, 1983; Feder and Wassersug, 1984; Burggren and Doyle, 1986; Burggren and Just, 1992; Orlando and Pinder, 1995; McKenzie and Taylor, 1996; Jia and Burggren, 1997a). This response is evident very soon after hatching in *X. laevis* and *Lithobates catesbeianus*, even before the degeneration of the external gills (Burggren and Doyle, 1986; Orlando and Pinder, 1995). However, buccal stroke volume is not responsive to hypoxia over the course of development (Feder and Wassersug, 1984). Larval anurans may also increase lung ventilation frequency, especially at extreme hypoxia (Feder and Wassersug, 1984; Burggren and Doyle, 1986).

In larval amphibians as well as fishes, neuroepithelial cells (NECs) located in the gills are thought to be the $O_2$-senstitive chemoreceptors involved in the hypoxic ventilatory responses (e.g. Jia and Burggren, 1997b; Burleson and Milsom, 1993; Straus et al., 2001; Jonz and Nurse, 2006; Milsom and Burleson, 2007), with sensory information being relayed from the gill arches via the cranial nerves IX and X (Burleson and Smatresk, 1990; Sundin and Nilsson, 2002). In almost all species examined, NECs appear in the gill filaments, although there are interspecific differences in distribution of the cells (Bailly et al., 1992; Coolidge et al., 2008). Some characteristics of NECs that suggest their role in $O_2$ sensing include abundant mitochondria, a well-developed Golgi complex, presence of dense-core vesicles and neurotransmitters, contact with nerve endings, and degranulation of dense core vesicles following acute hypoxic exposure (Dunel-Erb et al., 1982; Bailly et al., 1992; Goniakowska-Witalińska et al., 1993). In addition, chronic hypoxia induces NEC hypertrophy and extension of NEC membrane protrusions in adult zebrafish (Jonz et al., 2004).

During development, the earliest branchial NECs are observed at 5 dpf in larval zebrafish, and an increase in innervation of NECs has been correlated with an increase in ventilation frequency and sensitivity to hypoxia (Jonz and Nurse, 2005). In developing *X. laevis*, gill filaments start to form at 3 dpf (Nieuwkoop and Faber, 1967), but NECs have only been described in larvae after 7 dpf with relatively well-developed gills (Saltys et al., 2006).

In fast developing *X. laevis*, larvae have gone through more than 75% of the morphological stages in the first 3 weeks of development (total developmental time ~8 weeks, Nieuwkoop and Faber, 1967). However, most studies have focused on changes in gas exchanges and hypoxic responses approaching or during metamorphosis. The aim of this study was to explore the onset — in contrast to previous studies focused on the ongoing development — of the gill and lung ventilatory responses to acute aquatic hypoxia. Also investigated was the correlation of branchial 5-HT-IR NECs with early ventilatory responses. The effect of chronic hypoxic exposure on ventilatory responses to acute hypoxia and on 5-HT-IR NECs in the gill filaments was also studied. We hypothesized that the onset of ventilatory regulation is correlated with the development of 5-HT-IR NECs shortly after hatching, and that chronic hypoxia induces morphological changes in branchial 5-HT-IR NECs and modifies the early ventilatory responses to acute hypoxia.

## 2. Materials and methods

### 2.1. Animals

Adult *X. laevis* used for breeding were obtained from XENOPUS I (Ann Arbor, MI, USA). Adults were kept under a 14 h:10 h light/dark cycle at 22 ± 2 °C and fed daily with commercial frog food. To induce breeding, human chorionic gonadotropin (hCG, Sigma-Aldrich Corp., St. Louis, MO, USA) was injected into breeding pairs with a 1 mL syringe and a 26 gauge needle into the dorsal lymph sac, following standard breeding induction protocols. A total of eight breeding pairs, which produced 20 clutches of fertilized eggs, were used in the study. All animals use procedures were approved by the Institutional Animal Care and Use Committee.

### 2.2. Chronic exposure to hypoxia

Fertilized eggs obtained from breeding pairs were separated into two groups of approximately 120 eggs. Within 3 h post-fertilization, each group was placed in either a covered normoxic ($P_{O_2}$ of 150 mmHg) or hypoxic ($P_{O_2}$ of 110 mmHg) tank at a density of ~5 individuals·$L^{-1}$. A $P_{O_2}$ of 110 mmHg was selected because our pilot experiments with larval *Xenopus* indicated that this level of hypoxia was severe enough to elicit marked physiological responses in larvae (e.g. hyperventilation and tachycardia, unpublished), but not so severe as to prevent normal rates of development in a long-term experiment. Indeed, our goal was to examine the effects of a moderate level of hypoxia and the resultant more subtle effects that might emerge, rather than document the potentially teratogenic effects of severe hypoxia.

Incubation tanks were kept in a water bath maintained at 22 ± 1 °C. Larvae were fed daily with powder made from frog food followed by a water change. Water in the normoxic tank was kept aerated by bubbling with room air, and hypoxic water was equilibrated with a gas mixture of $N_2$ and air to produce a $P_{O_2}$ of 110 mmHg. $P_{O_2}$ in the gas mixture and water were measured with fiber-optic $O_2$ probes (Ocean Optic Inc., Dunedin, FL, USA), which were connected to a multifrequency phase fluorometer (MFPF-100, TauTheta Instruments LLC, Boulder, CO, USA). OOISensors software was used to obtain $P_{O_2}$ readings. Both aerial and aquatic $P_{O_2}$ in the hypoxic tank were kept at 110 mmHg during the entire incubation period.

### 2.3. Gill ventilation frequency

Measurements were made on both normoxic and hypoxic populations at 3, 5, 7, 10, 14 and 21 dpf, which corresponded to NF stages 42–44, 45–47, 48, 49, 50 and 51–52, respectively. Larvae on each developmental day were placed in a flow-through measurement chamber, which was modified from a 12-well cell culture dish. Each well was a cube (2.5 cm × 2.5 cm × 2.5 cm) with flat, transparent walls, allowing video recording from either side of the chamber for measurement of buccal pumping amplitude (described in section 2.4). Water of regulated $P_{O_2}$ at 22 ± 1 °C, flowed through at a rate of 75 mL·$min^{-1}$, a velocity sufficient to mix water around larvae and in the wells. The bottom of each water-filled well was filled with solidified 1.5% agarose gel. A smaller, central space for placement of an unanethetized larva was carved out from the agarose block. The size of the space was adjusted to accommodate larval body size. A piece of nylon mesh was then placed over the gel to confine the larva within the hollowed-out space. The measurement chamber with larval *X. laevis* was then transferred to the stage of an inverted microscope (TS-100, Nikon). Gill ventilatory responses to acute hypoxia were measured by direct observation at a total magnification of 40×.

At the beginning of each measurement, animals were placed in wells of the measurement chamber containing normoxic water ($P_{O_2}$ of 150 mmHg) for 30 min. After a first measurement in normoxic water, hypoxic water with a $P_{O_2}$ of 110 mmHg was introduced into the chamber. A 10-min period was provided for larvae to adjust before measurements were made. Normoxic water was then reintroduced for 10 min to avoid accumulated effects of acute hypoxia and the lack of access to air during the actual measurement period. This protocol was repeated for 70, 50 and 30 mmHg in sequence. Between each acute hypoxic exposure, water in the first and the last wells was sampled and measured with a fiber-optic $O_2$ probe to ensure that all larvae were exposed to the same $P_{O_2}$. After all the experimental procedures, including those described in Sections 2.4 and 2.5, larvae from both normoxic and hypoxic populations were weighed.

### 2.4. Buccal pumping amplitude

Buccal floor depression was measured as an index for buccal pumping amplitude (Feder and Wassersug, 1984). The measurement

chamber described in the previous subsection was used for confining larvae during recording. The head of a dissecting microscope was rotated by 90° to allow horizontal observation of the larva's side profile through the transparent holding chamber walls, and a video camera (Javelin Electronics, Japan) on the microscope was used to record buccal pumping behavior at 30 frames·s$^{-1}$. At least three consecutive video segments of 2–10 buccal pumping cycles, depending on acute $P_{O_2}$ level, were recorded. In a given ventilatory cycle, the distance between the top of the head and the bottom of the buccal floor was measured using Image-Pro software (Fig. 1A and B). The difference in distance between resting and maximal depression of the buccal floor was calculated as an index of buccal pumping amplitude.

### 2.5. Lung ventilation frequency and expired volume

Larvae were kept at 22 ± 1 °C in a 10-mL Erlenmeyer flask modified to accommodate a fiber-optic $O_2$ probe. Animals in the flask had free access to air and reduced $P_{O_2}$ in the water by their own metabolism, until aquatic $P_{O_2}$ dropped below 30 mmHg, at which partial pressure animals usually lose equilibrium. A video camera (HDR-SR1, Sony) was placed above the flask to record gas bubbles on the water surface expelled by larvae after taking air breaths. Lung ventilation frequency ($f_L$) was obtained by counting bubbles formed at each $P_{O_2}$ level in the video and calculated as breaths·h$^{-1}$ per animal. For lung ventilation volume, individual video frames of each air bubble (Fig. 1C) were taken from the videos and analyzed using Image-Pro software. From these images was obtained the radius of each air bubble allowing the calculation of the volume of each bubble, assuming the bubbles to be perfect spheres.

### 2.6. Immunofluorescent identification of 5-HT-IR NECs

Larvae were sacrificed by overdosing with MS-222 (Sigma-Aldrich, St. Louis, MO, USA) buffered to a pH of 7.4. Larvae were then fixed with 4% paraformaldehyde for 20 min at 4 °C, and the internal gills were removed and fixed for another 30 min at 4 °C. After washing in cold phosphate-buffered saline (PBS) containing (in mM) NaCl 137; $Na_2HPO_4$ 15.2; KCl 2.7 and $KH_2PO_4$ 1.5, at pH 7.4, fixed samples were then subjected to a blocking solution composed of 3% BSA and 1% triton in PBS at room temperature for 30 min. The whole gill sample was then incubated with a polyclonal rabbit primary antibody against serotonin (5-HT) (Sigma-Aldrich), which has been identified to label 5-HT-IR NECs in fish and larval *Xenopus* (Jonz and Nurse, 2003; Saltys et al., 2006), at a dilution of 1:100 in blocking solution at 4 °C overnight. Samples were washed several times in the blocking solution and then incubated with a goat anti-rabbit IgG secondary antibody conjugated with fluorescein at a dilution of 1:200 (Jackson ImmunoResearch Laboratories Inc., West Grove, PA, USA) for 1 h in dark at room temperature. The gills were then rinsed in PBS and mounted on microscope slides.

Whole-mount gill preparations were examined using an inverted microscope (Zeiss 200 M, Carl Zeiss Inc., Thornwood, NY, USA) and a confocal scanning system (CSU10, Yokogawa, Atlanta, GA, USA) equipped with an argon laser and a band pass 488/532 nm filter set to monitor fluorescein. Images obtained were analyzed using Image-Pro software to measure density and size of 5-HT-IR NECs in the gill filaments. Density was expressed as number of cells per filament length (in mm). Randomly selected cells were outlined and used for measurements of cell size. At least 100 cells were measured in the gills of each animal.

### 2.7. Statistical analysis

The overall effects of age, acute and chronic hypoxia on gill ventilation frequency, buccal pumping amplitude, lung ventilation frequency and expired volume were analyzed using three-way ANOVAs. Since the design of three-way ANOVA did not allow post-hoc comparisons between levels of age and of acute hypoxia within each chronic treatment group or between levels of acute and chronic hypoxia within age, additional two-way repeated measures ANOVAs were performed. Changes in NEC density and size, development measured by stage and body mass caused by age and chronic hypoxia were analyzed using two-way ANOVAs. If significant differences were seen ($P<0.05$), Tukey's multiple comparison tests were used to determine significance among acute and chronic $P_{O_2}$ at each stage or among stages in the normoxic group. All values are shown as mean ± 1 standard error from the mean.

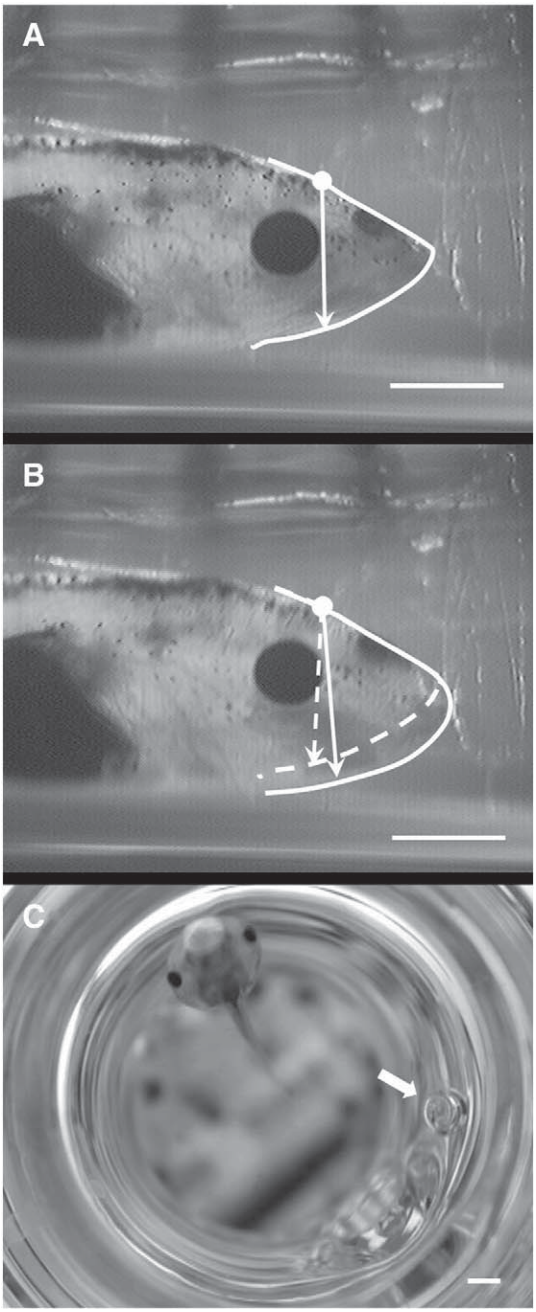


**Fig. 1.** Representative images of the lateral view of a larval *Xenopus laevis* at 7 dpf at the end of a buccal cycle (A) and during the phase of maximal buccal floor depression (B). In (A) and (B), the solid curve lines show the outlines of the head area. In (B), the dash curve line shows the position of the buccal floor in Panel A. The difference in distance between the solid (maximal depression) and the dash (end of a buccal cycle) arrowed lines in (B) was calculated as an index of buccal pumping amplitude. Note that the two arrowed lines are slightly rotated for presentation. Panel C shows a gas bubble (arrow) expelled by larva immediately after air breathing, with a second animal showing air-breathing behavior. The radius of the gas bubble was used to calculated volume of the bubble. Scale bars = 1 mm.

## 3. Results

### 3.1. Normoxic gill ventilation frequency and amplitude

Gill ventilation frequency ($f_G$) and buccal pumping amplitude in larvae raised and measured in normoxia were both highly dependent on development ($P<0.001$ for both variables). Larval *X. laevis* began gill ventilation at 3 dpf at a rate of $28\pm4$ beats·min$^{-1}$ (Fig. 2A). Gill ventilation frequency then increased as development progressed and peaked at 7 dpf at a rate of $48\pm3$ beats·min$^{-1}$, before gradually decreasing to approximately half of the highest rate at $22\pm3$ beats·min$^{-1}$ at 21 dpf. Unlike the complex pattern of developmental change in $f_G$, buccal pumping amplitude in normoxia increased throughout early development, with the amplitude of $0.27\pm0.01$ mm at 21 dpf being more than two times higher than the value of $0.12\pm0.02$ mm at 5 dpf (Fig. 2B).

### 3.2. Gill ventilatory responses to acute hypoxia in normoxic larvae

The first evidence of an acute hypoxic ventilatory response occurred at 3 dpf, with significant increase in $f_G$ ($P<0.001$). Moderate hypoxia ($P_{O_2}$ of 110 mmHg) had no effect on $f_G$ at 3 dpf, but more severe hypoxia ($P_{O_2}$ of 70 mmHg) caused a ~75% increase. Still lower $P_{O_2}$s (30 and 50 mmHg) induced an even greater increase of ~114% from the normoxic value (Fig. 2A). At 5 and 7 dpf, elevated $f_G$ in response to hypoxia generally followed a similar pattern to that of larvae at 3 dpf, although a more pronounced effect occurred at a $P_{O_2}$ of 70 mmHg at 7 dpf. Sensitivity to acute hypoxia at the level of $P_{O_2}$ of 110 mmHg increased further at 10 and 14 dpf, since acute exposure to this $P_{O_2}$ elicited a similar response to all other lower $O_2$ levels (Fig. 2A). At 21 dpf, buccal pumping frequency in response to hypoxia was again more muted, and moderate hypoxia failed to stimulate $f_G$. However, the ventilatory frequency response to $P_{O_2}<70$ mmHg remained two to three times higher than resting frequency.

Acute hypoxia also caused an increase in buccal amplitude. However, this effect was relatively small and only seen when the whole data set, including both normoxic and hypoxic populations, was analyzed using three-way ANOVA ($P<0.001$). Acute hypoxia had no effect on buccal amplitude in the normoxic population alone ($P=0.164$).

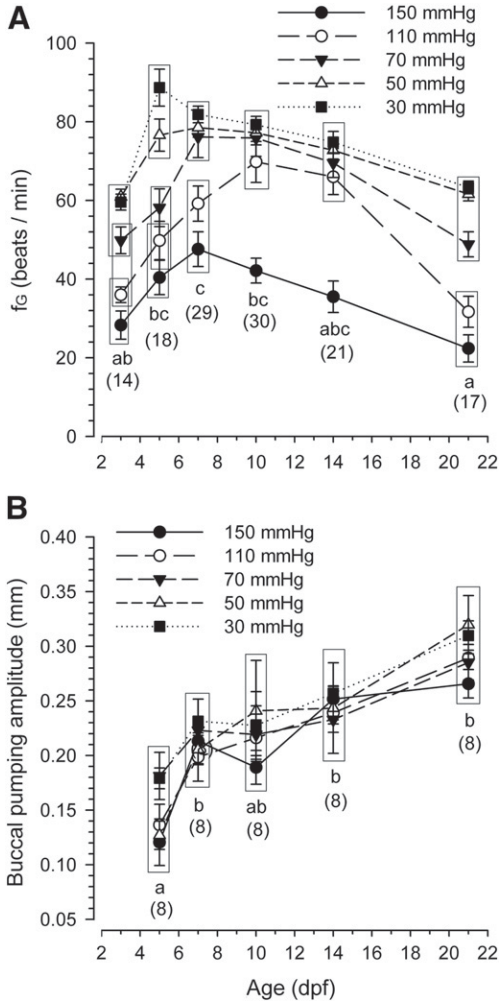


**Fig. 2.** Gill ventilation frequency ($f_G$) (A) and buccal pumping amplitude (B) of normoxic larvae of *Xenopus laevis* as a function of age at five levels of acute hypoxic exposure. Mean values ± SE are plotted. *n* in parentheses. Different letters indicate statistical difference of normoxic ventilation frequency and amplitude (solid line) between ages. Boxes enclose statistically identical means among levels of acute hypoxic exposure at each age. See results for statistical assessment.

### 3.3. Normoxic lung ventilation frequency and expired volume

Larval development also highly influenced normoxic $f_L$ and volume of the exhaled gas bubble ($P<0.001$ for both variables). The earliest use of air by larvae from the normoxic populations occurred at 3 dpf, but on this day, $f_L$ was less than 1 breath·h$^{-1}$ (Fig. 3A). As development progressed, $f_L$ increased to $3\pm1$ breaths·h$^{-1}$ at 5 dpf, and remained constant until larvae reached 21 dpf, at which point

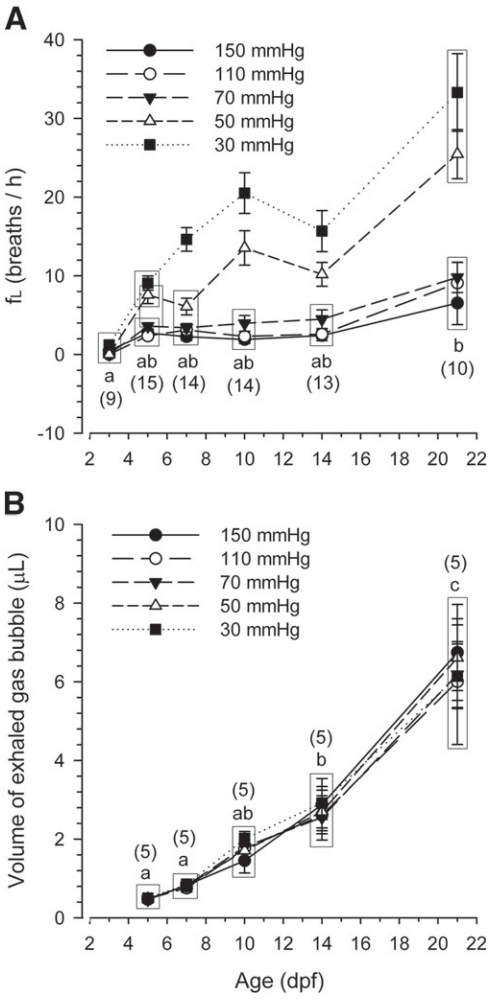


**Fig. 3.** Lung ventilation frequency ($f_L$) (A) and volume of exhaled gas bubbles (B) of normoxic larvae of *Xenopus laevis* as a function of age at five $O_2$ levels of acute exposure. See Fig. 2 for plotting convention.

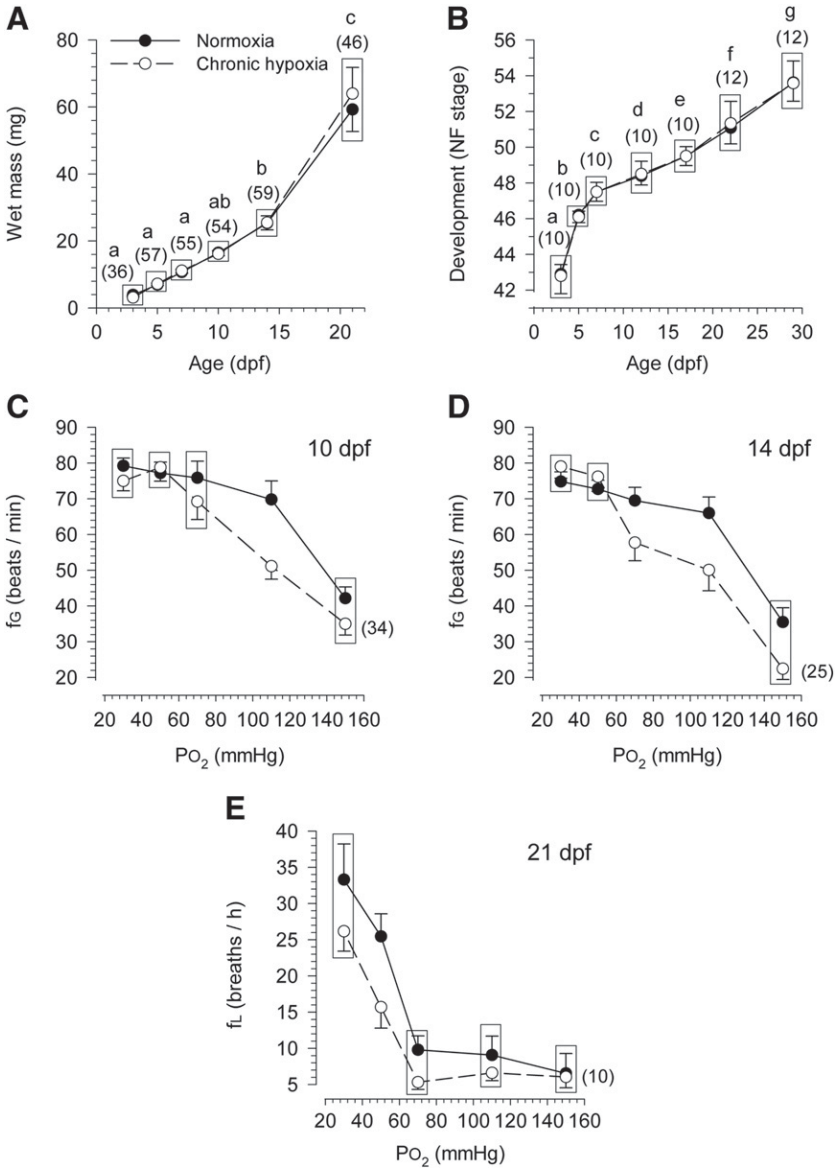


**Fig. 4.** Effects of chronic hypoxia at a $P_{O_2}$ of 110 mmHg (open circles) on wet mass (A), development (B) as a function of age, and on gill ventilation frequency ($f_G$) (C) and (D) and lung ventilation frequency ($f_L$) (E) as a function of levels of acute hypoxic exposure. Note that only selected stages at which larval hypoxic ventilatory responses are modified by the chronic exposure to hypoxia are shown. *n* equal in each chronic treatment group in (A) and (B) and in parentheses. From (C) to (E), *n* of hypoxic larvae in parentheses. See Fig. 2 for plotting convention.

lung breathing rate more than doubled to $7 \pm 3$ breaths·h$^{-1}$ (Fig. 3A). In contrast to the relatively constant $f_L$ during early development, larval normoxic lung expired volume increased from $0.47 \pm 0.03$ μL at 5 dpf to $2.88 \pm 0.66$ μL at 14 dpf. The value then showed a sharp increase to $6.74 \pm 1.89$ μL at 21 dpf (Fig. 3B).

### 3.4. Lung ventilatory response to hypoxia in normoxic larvae

Pulmonary hyperventilation in response to hypoxia started by 5 dpf, increasing from about 3 breaths·h$^{-1}$ at normoxia to 9 breaths·h$^{-1}$ at the $P_{O_2}$ of 30 mmHg (Fig. 3A). The magnitude of this response continued to increase throughout subsequent stages examined, with the highest magnitude of increase found at 21 dpf, from a normoxic value of $7 \pm 3$ to $33 \pm 5$ breaths·h$^{-1}$ at a $P_{O_2}$ of 30 mmHg. Despite the enhanced response during development, larvae at all stages only increased $f_L$ when aquatic $P_{O_2}$ had dropped below 50 mmHg. In contrast, lung expired volume was independent of ambient $P_{O_2}$ (Fig. 3B).

### 3.5. Larval development and growth in chronic hypoxia

Larval development was categorized according to their increases in wet mass during development as well as morphological changes. Larval wet mass remained constant between 3 and 7 dpf, followed by an increase from 10 dpf to the last stage examined (Fig. 4A). A sharp increase in body mass was observed especially between 14 and 21 dpf (Fig. 4A). In our laboratory conditions, larvae progressed through stages as described in the NF staging system (Fig. 4B) (Nieuwkoop and Faber, 1967). However, neither body mass nor the time to advance to the next stage was significantly affected by chronic exposure to a $P_{O_2}$ of 110 mmHg (Fig. 4A and B), even though physiological changes were observed (see below).

### 3.6. Acute ventilatory responses in chronically hypoxic larvae

Chronic exposure to hypoxia ($P_{O_2}$ of 110 mmHg) induced only modest overall changes in $f_G$ ($P<0.001$) and $f_L$ ($P=0.01$) compared to

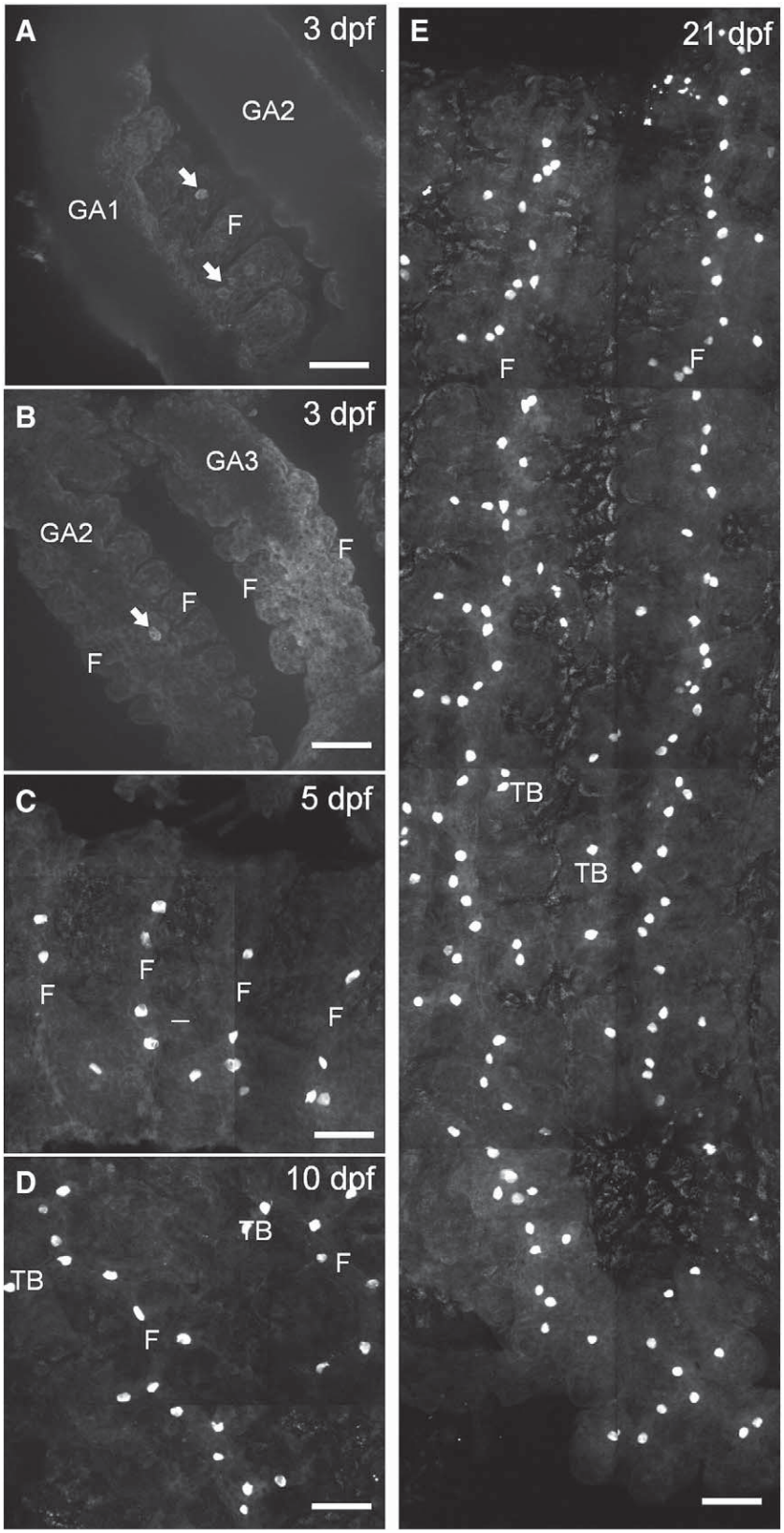


**Fig. 5.** Serotonin-immunoreactive neuroepithelial cells (5-HT-IR NECs) on gill filaments (F) and respiratory terminal branches (TB) at 3 dpf (A and B), 5 dpf (C), 10 dpf (D) and 21 dpf (E) in *Xenopus laevis*. In (A) and (B), 5-HT-IR NECs (arrows) were identified on developing gill filament on gill archs 1, 2 and 3 (GA1, GA2 and GA3). In Panel D, TB have formed and 5-HT-IR NECs are evident on these structures at 10 dpf. At 21 dpf (Panel E), 5-HT-IR NECs were located along the axis of filaments and on TB. Scale bars = 50 μM.

control populations. Surprisingly, there was no difference in normoxic ventilation values between populations at any of the dpf measured in the study. Yet, in both 10- and 14-day-old larvae, chronic hypoxia attenuated $f_G$ at a $P_{O_2}$ of 110 mmHg, and decreased frequency was also observed at a $P_{O_2}$ of 70 mmHg at 14 dpf (Fig. 4C and D). However, acute hypoxic responses at $P_{O_2}$ of 30 and 50 mmHg were not affected.

Compared to $f_G$, the effect of chronic hypoxia on $f_L$ was even less apparent, with lung breathing frequency affected only at a $P_{O_2}$ of 50 mmHg at 21 dpf, at which hypoxic larvae showed a lower value, $16 \pm 3$ than $25 \pm 3$ breaths·h$^{-1}$ in the normoxic population (Fig. 4E).

Gill and lung ventilation amplitude and expired volume were not different between normoxic and chronically hypoxic populations measured at any $P_{O_2}$ at any day of development.

### 3.7. Neuroepithelial cells: ontogeny and chronically hypoxic effects

Larval *X. laevis* possess four gill arches with one row of filaments on the first and fourth gill arches, and two rows of filaments on the second and third arches (Minnich et al., 2002). During early development, filaments appeared on gill arches 1–3 at 3 dpf (Fig. 5A and B). 5-HT-IR NECs were first visualized during this early period of development (Fig. 5A and B). NEC density was $15 \pm 1$ cells·mm of filament$^{-1}$ at 5 dpf through 7 dpf, with an increase at 10 dpf to $29 \pm 2$ cells·mm of filament$^{-1}$ (Figs. 5C, D and 6A). At this point in development, gill filament branching occurred and 5-HT-IR NECs ($16 \pm 2\%$) were first identified on the respiratory terminal branches (TB) of the gills (Figs. 5D and 6A). Density of 5-HT-IR NECs reached the highest value at 14 and 21 dpf, at $37 \pm 2$ and $45 \pm 3$ cells·mm of filament$^{-1}$, respectively (Fig. 6A). At these two later stages, with further development and branching of the gills, more cells (approximately 32–38%, Fig. 6A) were found on TB, especially at the most distal end of filaments. Unlike the strong developmental effect on density ($P<0.001$), chronic hypoxic exposure had no significant effect on 5-HT-IR NEC density.

Beyond 3 dpf, 5-HT-IR NECs generally appeared in a linear fashion along the central axis of the gill filaments, with some located on the TB starting from 10 dpf (Fig. 5). In the filament, 5-HT-IR NECs were found on the apical side where the main fold venules that carry oxygenated blood return to the atrium (Minnich et al., 2002).

NEC size was not significantly affected by development, ranging from $75 \pm 3$ μm$^2$ at 5 dpf to $66 \pm 2$ μm$^2$ at 21 dpf. However, in larvae exposed to chronic hypoxia, 5-HT-IR NECs ($77 \pm 2$ μm$^2$) were significantly larger than the control animals at 21 dpf (Fig. 6B).

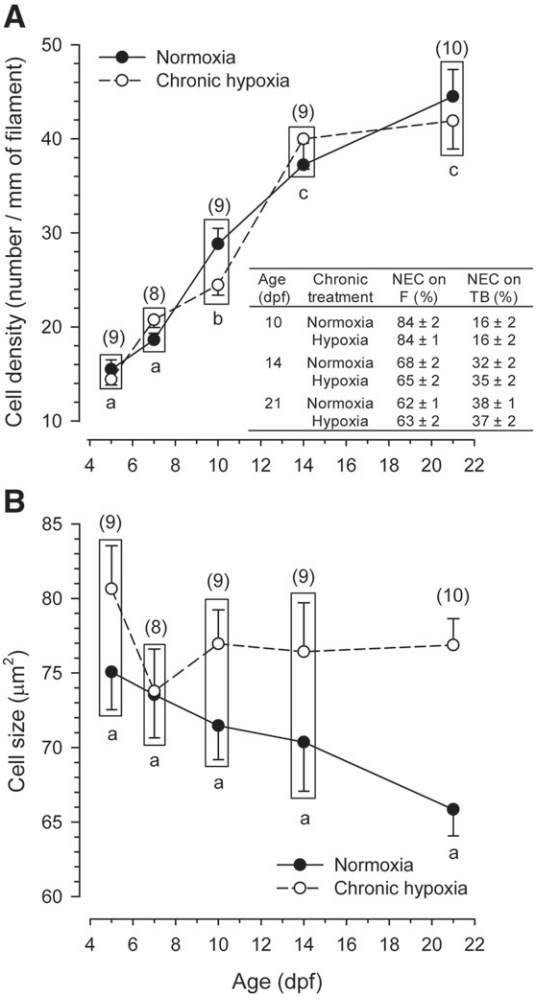


**Fig. 6.** Density (A) and size (B) of serotonin-immunoreactive neuroepithelial cells as a function of age in the normoxic (solid circles) and the chronically hypoxic (open circles) larvae of *Xenopus laevis*. Table in Panel A shows relative density of neuroepithelial cells (NEC) on gill filaments (F) and respiratory terminal branches (TB) at 10, 14 and 21 dpf. *n* equal in each chronic treatment group and in parentheses. See Fig. 2 for plotting convention.

## 4. Discussion

### 4.1. Ontogeny of normoxic gill and lung ventilation

Very early in development (3 dpf), the gills of *X. laevis* are still external, and movement of the buccal cavity appears to only create ill-defined water movement around the gills, rather than irrigating them directly and efficiently, a condition also occurring in newly hatched bullfrogs (Burggren and Doyle, 1986). The onset of lung ventilation also started at 3 dpf, at a very low and erratic rate. Then frequency increased to and was maintained at about 2–3 breaths·h$^{-1}$ at normoxia during the first 14 days of development (Fig. 3A). Unlike the relatively constant $f_L$, normoxic $f_G$ in *X. laevis* gradually increased until 7 dpf (Fig. 2A), which may reflect an increase in the total number of 5-HT-IR and development of structures related to the buccal pumping mechanism, such as the levator and dilator muscles (Gargaglioni and Milsom, 2007). The subsequent decrease in $f_G$ after 7 dpf concurrent with increases in both normoxic $f_L$ and lung expired volume between 14 and 21 dpf (Fig. 3A), indicates the transition of the relative importance of the gills and lungs in gas exchange. However, one should note that cutaneous gas exchange was not measured in our study. The skin is still responsible for more than half of the total gas exchange after the gradual emergence of lung ventilation, at least in larval *Lithobates catesbeianus* (Burggren and West, 1982).

Despite the decrease in $f_G$ between 14 and 21 dpf, the internal gills are still developing even after this period of development (Minnich et al., 2002). In addition, our measure of buccal floor depression, which is directly proportional to buccal stroke volume (Feder and Wassersug, 1984), increased during early development (Fig. 2B). This suggests that buccal stroke volume per minute may remain constant, if not increase, despite the decrease in $f_G$. Since larval *Xenopus* are suspension feeders, the primary role of the internal gills may switch from a sole gas exchanger to a filter for food particles after the gradual emergence of the air-breathing behavior. An increased gill irrigation volume following a sharp increase in body mass (Fig. 4B) during this period of development may be important for capturing an adequate amount of food from the environment.

### 4.2. Ontogeny of acute hypoxic gill and lung ventilatory responses

When gill hypoxic hyperventilation first started at 3 dpf, acute $P_{O_2}$ stimulus of 70 mmHg or lower was necessary to initiate a response (Fig. 2A). Hypoxic sensitivity increased at 7 dpf and then again at 10 dpf, at which a moderate level of hypoxia ($P_{O_2}$ of 110 mmHg) had the same stimulatory effect as lower $O_2$ levels (Fig. 2A). Pulmonary ventilatory reflexes in hypoxia were established at 5 dpf, about 2 days after the appearance of branchial hypoxic response, and the magnitude of the response increased as development progressed, especially between 14 and 21 dpf (Fig. 3A). This implies that not only the transition of normoxic gill and lung respiration but also that the transition of $f_G$ and $f_L$ responses to hypoxia takes place during this

period of development. Despite the gradual increase in pulmonary hypoxic sensitivity during development, the $P_{O_2}$ required to stimulate pulmonary hyperventilation remained at ~50 mmHg in all stages examined (Fig. 3A). The same level of $O_2$ also caused a maximal magnitude of increase in $f_G$ throughout the stages examined (Fig. 2A). Collectively, these data suggest that at this relatively low $O_2$ level, the highest rate at which larvae can ventilate their gills has been reached, and larvae must start to rely more on air as the source of $O_2$. In addition, a high $f_G$ at a very low ambient $P_{O_2}$ could potentially cause larvae to lose $O_2$ from blood in the gills and skin into the ambient water (West and Burggren, 1982; Feder and Wassersug, 1984). The combination of an early development of pulmonary hypoxic hyperventilation and a capped degree of increase in $f_G$ may help limit branchial $O_2$ loss at severe hypoxia.

Given the putative role of NECs on $O_2$ sensing (Dunel-Erb et al., 1982; Jonz et al., 2004; Burleson et al., 2006), the measured increase in density of 5-HT-IR cells concomitant with enhanced $f_G$ responses at 10 dpf (Fig. 6A) may explain the developmental increase in hypoxic sensitivity. However, the increase in cell density failed to correlate with $f_L$ response to acute hypoxia, which might be due to a different stimulation threshold for the gill and lung central pattern generator (CPG), or a late maturation of the lung CPG in development (Torgerson et al., 1997).

Unlike the strong hypoxia-driven increase in $f_G$ and $f_L$, buccal pumping amplitude and lung expired volume showed little response to similar levels of acute hypoxia in *X. laevis*, as has been previously reported (Feder and Wassersug, 1984), suggesting ventilatory pumps with a flexible rate but a constant volume at hypoxia during early development. Yet, bullfrog larvae show strong $O_2$-dependent increase total branchial water flow and buccal pressure (Jia and Burggren, 1997a). Either interspecific differences in larval hypoxic response or different methods between studies could account for the difference between *Xenopus* and *Lithobates*. Indeed, due to the small size of larval *X. laevis*, a direct measurement of buccal pressure or total branchial water flow is difficult. Our imaging approach to measure only takes changes in vertical distance into consideration, and may not be sensitive enough to detect changes in ventilatory amplitude, which may be rather modest during acute hypoxic exposure.

### 4.3. Chronic hypoxia-induced changes in development, growth and acute ventilatory responses

Development and growth measured by wet mass were not affected by moderate chronic hypoxia (110 mmHg, Fig. 4A and B). Similar findings of normal growth in hypoxia have been reported in *X. laevis* (Territo and Altimiras, 1998) and other amphibian species, including *Rana sphenocephala* and *palustris* (Mills and Barnhar, 1999) and *Ambystoma maculatum* and *annulatum* (Mills and Barnhar, 1999; Valls and Mills, 2007). However, far lower $PO_2$s, chronic (~30 mmHg) and intermittent (45 mmHg, 12 $h \cdot day^{-1}$) hypoxia delay development in *Ambystoma* (Mills and Barnhar, 1999; Valls and Mills, 2007) and *Lithobates catesbeianus* (Simard et al., 2003), respectively. In a terrestrial anuran, *Pseudophryne bibroni*, even moderate hypoxia at a $PO_2$ around 100 mmHg slows embryonic development and increases the time to hatching (Bradford and Seymour, 1988). Collectively, these studies suggest that ambient $O_2$ level plays a more important role on early development of species with a terrestrial life cycle.

Chronic exposure to a $P_{O_2}$ of 110 mmHg decreased the magnitude of $f_G$ and $f_L$ responses to acute hypoxia at later stages examined (Fig. 4C–E). Despite lower $f_G$ at acute $PO_2$s of 70 and 110 mmHg, larvae showed similar responses at lower $P_{O_2}$, showing that the sensitivity to more severe hypoxia was not changed by chronic exposure to hypoxia. Unlike $f_G$, $f_L$ was unaltered by the chronic hypoxic incubation except for an acute $P_{O_2}$ of 50 mmHg at 21 dpf (Fig. 4E). There is a paucity of information about the effect of chronic hypoxia on the ventilatory reflexes during very early development in lower vertebrates. In one of the few such studies, Vulesevic and Perry (2006) exposed zebrafish larvae to severe hypoxia ($P_{O_2}$ of 30–40 mmHg) for the first 7 dpf and measured their ventilatory response to hypoxia when the fish subsequently reached maturity. In another study, larval bullfrogs were exposed to intermittent hypoxia ($P_{O_2}$ of 45 mmHg) 12 $h \cdot day^{-1}$ for 2 weeks (Simard et al., 2003) before hypoxic ventilatory responses were examined. The hypoxic populations in both studies showed no difference in their hypoxic ventilatory response. Differences in experimental procedures, levels of chronic exposure and stages of animals subjected to long-term exposure make it difficult to compare the results. A common observation seems to be that development of hypoxic ventilatory control is not altered by a chronic (pre)exposure to hypoxia. However, changes in ventilatory regulation may still be induced by long-term exposure to a more extreme $P_{O_2}$ and has not been investigated.

### 4.4. Ontogeny of branchial neuroepithelial cells

Little is known of the early development of NECs in aquatic vertebrates. In the present study, 5-HT-IR NECs were detected in the developing gill filament buds at 3 dpf, a stage at which gill ventilation and hypoxic branchial hyperventilation has also started (Figs. 2A, 5A and B). 5-HT-IR NECs first appear on the gill arches in zebrafish at 3 dpf and then on 5 dpf when the branchial filaments appear, which also corresponds with the first appearance of hypoxic stimulation of branchial ventilation (Jonz and Nurse, 2005). Thus, the ontogeny of branchial 5-HT-IR NECs and their putative role in $O_2$ chemoreception related to hypoxic ventilatory responses appears to take similar developmental time courses in these two lower vertebrates.

In larval *X. laevis*, the density of 5-HT-IR NECs started to increase almost immediately after the first appearance of these cells and was significantly different at 10 dpf, which corresponds to the period when an elevated hypoxic ventilatory response develops (Figs. 2A and 3A). This contrasts with the previous report (Saltys et al., 2006) of no change in NEC density with development from “pre-metamorphic” to “pro-metamorphic” *X. laevis*, although pro-metamorphic larvae are beyond the stages examined in our study. Another possibility causing the difference may be due to differences in density measurement and calculation between studies. In the present study, density was calculated as the number of cells·mm of filament$^{-1}$ instead of cells·$\mu m^2$ of filament$^{-1}$ as in the other study (Saltys et al., 2006). The increase in cell density seen here is very possibly due to the appearance of the TB at 10 dpf and 5-HT-IR NECs in these structures (Fig. 5D) in addition to differentiation of cells along the central axis of the gill filaments. However, with either way of calculation, the total number of NECs in the gills increases as development progresses due to either a longer filament or larger area of gill tissues in older larvae than the earlier ones.

In addition to zebrafish and the clawed frog, NECs have been described in the gills of several other species of fish (Dunel-Erb et al., 1982; Bailly et al., 1992; Jonz and Nurse, 2003; Zaccone et al., 2006; Coolidge et al., 2008) and larval and neotenic amphibians (Goniakowska-Witalińska et al., 1993; Saltys et al.;, 2006). In fish, NECs are separated from the environment by the thin gill epithelium in gill filaments, and the specific location of NECs within filaments is near the efferent vasculature (Dunel-Erb et al., 1982; Bailly et al., 1992; Jonz and Nurse, 2003; Burleson, 2009). In the current study, 5-HT-IR NECs were observed on the venules side of the filament carrying oxygenated blood back to the left atrium and on the respiratory terminals. These locations are consistent with those in fish (Dunel-Erb et al., 1982; Bailly et al., 1992; Jonz and Nurse, 2003) and may make them ideal for sensing $P_{O_2}$ in both the water and blood.

### 4.5. Chronic hypoxia-induced changes in branchial neuroepithelial cells

In comparison to the findings of a lack of difference in 5-HT-IR NEC density using adult zebrafish exposed to a chronic $P_{O_2}$ of 30–35 mmHg (Jonz et al., 2004; Vulesevic et al., 2006), it is not

surprising that 5-HT-IR NEC density remain constant in our study (Fig. 6A). However, in one of the studies, density of NECs labeled with synaptic vesicle protein but not expressing 5-HT increases in chronically hypoxic zebrafish (Jonz et al., 2004). The function of 5-HT-negative NECs is still uncertain, but it is possible that the density of these cells could also be modified by chronic hypoxia in larval *Xenopus*. Unlike cell density, the difference in cell size between the control and chronically hypoxic groups became more significant as development progressed (Fig. 6B). Larger branchial NECs have also been reported in adult zebrafish (Jonz et al., 2004). As suggested in their study, the increase in size may be related to a higher surface area and more complex shape of the cells, which could increase the production of synaptic vesicles and enhance the release of 5-HT or other neurotransmitters to the postsynaptic neurons. Increased 5-HT-IR NEC size may also allow for more abundant mitochondria and/or a more developed Golgi apparatus that are required for energy production and protein synthesis during $O_2$ chemoreception at an environment with lower $O_2$ availability, which may explain a maintained normoxic ventilation in the control and hypoxic larvae.

## 5. Conclusions

This study demonstrates that both gill and lung ventilatory reflexes in *X. laevis* begin within a day of hatching, and a possible transition of the relative importance of the gills and lungs on gas exchange happens between 14 and 21 dpf, corresponding to the increase in lung expired volume and the onset of blood perfusion in the lungs. During ontogeny of the ventilatory reflex, sensitivity to more severe hypoxia develops first, and then to moderate hypoxia appears later, which we hypothesize is associated with the increase in 5-HT-IR NEC density during development. The effects of chronic moderate hypoxia involve stimulation of 5-HT-IR NEC cell size and modification of larval acute ventilatory responses to hypoxia at later stages examined. Our study suggests a conserved ontogeny of the role of 5-HT-IR NECs on development of the ventilatory response in larval fish and anuran amphibians. However, a more complex ventilatory regulation appears in air-breathing amphibians with the gradual emergence of the lungs later in development. The role of the gill and lung central pattern generators on the different gill and lung ventilatory responses to hypoxia deserves further study, as do the effects of hypoxia in the air, water or a combination of these media on the ontogeny of lung development.

## Acknowledgements

This study was supported by the US NSF operating grant 0614815. The authors thank Dr. Lon Turnbull for the assistance with confocal microscopy.

## References

Bailly, Y., Dunel-Erb, S., Laurent, P., 1992. The neuroepithelial cells of the fish gill filament: indolamine-immunocytochemistry and innervation. Anat. Rec. 233, 143–161.

Bradford, D.F., Seymour, R.S., 1988. Influence of environmental $Po_2$ on embryonic oxygen consumption, rate of development, and hatching in the frog *Pseudophryne bibroni*. Physiol. Zool. 61, 475–482.

Burggren, W.W., Doyle, M., 1986. Ontogeny of regulation of gill and lung ventilation in the bullfrog, *Rana catesbeiana*. Respir. Physiol. 66, 279–291.

Burggren, W.W., Just, J.J., 1992. Developmental changes in amphibian physiological systems. In: Feder, M.E., Burggren, W.W. (Eds.), Environmental Physiology of the Amphibia. University of Chicago Press, Chicago, pp. 467–530.

Burggren, W.W., Pan, T.-C., 2009. Chemoreceptive control of ventilation in amphibians and air-breathing fishes. In: Zaccone, G., Cutz, E., Adriaensen, D., Nurse, C.A. (Eds.), Structure, evolution and function of the airway chemoreceptors in the vertebrates. Science Publishers, Enfield, NH, pp. 151–183.

Burggren, W.W., Warburton, S.J., 2007. Amphibians as animal models for laboratory research in physiology. ILAR J. 48, 260–269.

Burggren, W.W., West, N.H., 1982. Changing respiratory importance of gills, lungs, and skin during metamorphosis in the bullfrog *Rana catesbeiana*. Respir. Physiol. 47, 151–164.

Burleson, M.L., 2009. Sensory innervation of the gills: $O_2$-sensitive chemoreceptors and mechanoreceptors. Acta Histochem. 111, 196–206.

Burleson, M.L., Milsom, W.K., 1993. Sensory receptors in the first gill arch of rainbow trout. Respir. Physiol. 93, 97–110.

Burleson, M.L., Smatresk, N.J., 1990. Effects of sectioning cranial nerves IX and X on cardiovascular and ventilatory reflex responses to hypoxia and NaCN in channel catfish. J. Exp. Biol. 154, 407–420.

Burleson, M.L., Mercer, S.E., Wilk-Blaszczak, M.A., 2006. Isolation and characterization of putative $O_2$ chemoreceptor cells from the gills of channel catfish (*Ictalurus punctatus*). Brain Res. 1092, 100–107.

Coolidge, E.H., Ciuhandu, C.S., Milsom, W.K., 2008. A comparative analysis of putative oxygen-sensing cells in the fish gill. J. Exp. Biol. 211, 1231–1242.

Dunel-Erb, S., Bailly, Y., Laurent, P., 1982. Neuroepithelial cells in fish gill primary lamellae. J. Appl. Physiol. 53, 1342–1353.

Feder, M.E., 1983. Responses to acute aquatic hypoxia in larvae of the frog *Rana berlandieri*. J. Exp. Biol. 104, 79–95.

Feder, M.E., Burggren, W.W., 1987. Skin breathing in vertebrates. Sci. Am. 253, 126–143.

Feder, M.E., Wassersug, R.J., 1984. Aerial versus aquatic oxygen consumption in larvae of the clawed frog, *Xenopus laevis*. J. Exp. Biol. 108, 231–245.

Feder, M.E., Seale, D.B., Boraas, M.E., Wassersug, R.J., Gibbs, A.G., 1984. Functional conflicts between feeding and gas exchange in suspension-feeding tadpoles, *Xenopus laevis*. J. Exp. Biol. 110, 91–98.

Gargaglioni, L.H., Milsom, W.K., 2007. Control of breathing in anuran amphibians. Comp. Biochem. Physiol. A: Mol. Integr. Physiol. 147, 665–684.

Goniakowska-Witalińska, L., Zaccone, G., Fasulo, S., 1993. Immunocytochemistry and ultrastructure of the solitary neuroepithelial cells in the gills of the neotenic tiger salamander *Ambystoma tigrinum* (Urodela, Amphibia). Eur. Arch. Biol. 104, 45–50.

Jia, X.X., Burggren, W.W., 1997a. Developmental changes in chemoreceptive control of gill ventilation in larval bullfrogs (*Rana catesbeiana*). I. Reflex ventilatory responses to ambient hyperoxia, hypoxia and NaCN. J. Exp. Biol. 200, 2229–2236.

Jia, X.X., Burggren, W.W., 1997b. Developmental changes in chemoreceptive control of gill ventilation in larval bullfrogs (*Rana catesbeiana*). II. Sites of $O_2$-sensitive chemoreceptors. J. Exp. Biol. 200, 2237–2248.

Jonz, M.G., Nurse, C.A., 2003. Neuroepithelial cells and associated innervation of the zebrafish gill: a confocal immunofluorescence study. J. Comp. Neurol. 461, 1–17.

Jonz, M.G., Nurse, C.A., 2005. Development of oxygen sensing in the gills of zebrafish. J. Exp. Biol. 208, 1537–1549.

Jonz, M.G., Nurse, C.A., 2006. Ontogenesis of oxygen chemoreception in aquatic vertebrates. Respir. Physiol. Neurobiol. 154, 139–152.

Jonz, M.G., Fearson, I.M., Nurse, C.A., 2004. Neuroepithelial oxygen chemoreceptors of the zebrafish gill. J. Physiol. 560, 737–752.

Kinkead, R., 2009. Phylogenetic trends in respiratory rhythmogenesis: insights from ectothermic vertebrates. Respir. Physiol. Neurobiol. 168, 39–48.

Malvin, G.M., 1989. Gill structure and function: amphibian larvae. In: Wood, S.C. (Ed.), Comparative Pulmonary Physiology: Current Concepts. : Lung Biology in Health and Disease., Vol. 39. Marcel Dekker, Inc, New York, pp. 121–151.

McKenzie, D.J., Taylor, E.W., 1996. Cardioventilatory responses to hypoxia and NaCN in the neotenous axolotl. Respir. Physiol. 106, 255–262.

Mills, N.E., Barnhar, M.C., 1999. Effects of hypoxia on embryonic development in two *Ambystoma* and two *Rana* species. Physiol. Biochem. Zool. 72, 179–188.

Milsom, W.K., Burleson, M.L., 2007. Peripheral arterial chemoreceptors and the evolution of the carotid body. Respir. Physiol. Neurobiol. 157, 4–11.

Minnich, B., Bartel, H., Lametschwandtner, A., 2002. How a highly complex three-dimensional network of blood vessels regresses: the gill blood vascular system of tadpoles of *Xenopus* during metamorphosis. A SEM study on microvascular corrosion casts. Microvasc. Res. 64, 425–437.

Nieuwkoop, P.D., Faber, J., 1967. Normal table of *Xenopus laevis* (Daudin). North-Holland Publishing, Amsterdam.

Orlando, K., Pinder, A.W., 1995. Larval cardiorespiratory ontogeny and allometry in *Xenopus laevis*. Physiol. Biochem. Zool. 68, 63–75.

Pronych, S., Wassersug, R.J., 1994. Lung use and development in *Xenopus laevis* tadpoles. Can. J. Zool. 72, 738–743.

Saltys, H.A., Jonz, M.G., Nurse, C.A., 2006. Comparative study of gill neuroepithelial cells and their innervation in teleosts and *Xenopus* tadpoles. Cell Tissue Res. 323, 1–10.

Simard, E., Trépanier, G., Larochelle, J., Kinkead, R., 2003. Intermittent hypoxia and plasticity of respiratory chemoreflexes in metamorphic bullfrog tadpoles. Respir. Physiol. Neurobiol. 135, 59–72.

Straus, C., Wilson, R.J., Remmers, J.E., 2001. Oxygen sensitive chemoreceptors in the first gill arch of the tadpole, *Rana catesbeiana*. Can. J. Physiol. Pharmacol. 79, 959–962.

Sundin, L., Nilsson, S., 2002. Branchial innervation. J. Exp. Zool. 293, 232–248.

Territo, P.R., Altimiras, J., 1998. The ontogeny of cardio-respiratory function under chronically altered gas compositions in *Xenopus laevis*. Respir. Physiol. 111, 311–323.

Torgerson, C.S., Gdovin, M.J., Remmers, J.E., 1997. Ontogeny of central chemoreception during fictive gill and lung ventilation in an *in vitro* brainstem preparation of *Rana catesbeiana*. J. Exp. Biol. 200, 2063–2072.

Valls, J.H., Mills, N.E., 2007. Intermittent hypoxia in eggs of *Ambystoma maculatum*: embryonic development and egg capsule conductance. J. Exp. Biol. 210, 2430–2435.

Vulesevic, B., Perry, S.F., 2006. Developmental plasticity of ventilatory control in zebrafish, *Danio rerio*. Respir. Physiol. Neurobiol. 154, 396–405.

Vulesevic, B., McNeill, B., Perry, S.F., 2006. Chemoreceptor plasticity and respiratory acclimation in the zebrafish Danio rerio. J. Exp. Biol. 209, 1261–1273.

Wang, T., Hedrick, M.S., Ihmied, Y.M., Taylor, E.W., 1999. Control and interaction of the cardiovascular and respiratory systems in anuran amphibians. Comp. Biochem. Physiol. A: Mol. Integr. Physiol. 124, 393–406.

Wassersug, R.J., Feder, M.E., 1983. The effects of aquatic oxygen concentration, body size and respiratory behaviour on the stamina of obligate aquatic (*Bufo americanus*) and facultative air-breathing (*Xenopus laevis* and *Rana berlandieri*) anuran larvae. J. Exp. Biol. 105, 173–190.

Wassersug, R.J., Murphy, A.M., 1987. Aerial respiration facilitates growth in suspension-feeding anuran larvae (*Xenopus laevis*). Exp. Biol. 46, 141–147.

West, N.H., Burggren, W.W., 1982. Gill and lung ventilation responses to steady-state aquatic hypoxia and hyperoxia in the bullfrog tadpole. Respir. Physiol. 47, 165–176.

Zaccone, G., Mauceri, A., Fasulo, S., 2006. Neuropeptides and nitric oxide synthase in the gill and the air-breathing organs of fishes. J. Exp. Zool. 305A, 428–439.